Carbohydrate Polymers 264 (2021) 118010

Contents lists available at ScienceDirect

Carbohydrate Polymers

journal homepage: www.elsevier.com/locate/carbpol

Are all ulvans equal? A comparative assessment of the chemical and gelling properties of ulvan from blade and filamentous *Ulva*

Joel T. Kidgell [a,*], Susan M. Carnachan [b], Marie Magnusson [c], Rebecca J. Lawton [c], Ian M. Sims [b], Simon F.R. Hinkley [b], Rocky de Nys [a], Christopher R.K. Glasson [c]

[a] MACRO – The Centre for Macroalgal Resources and Biotechnology, College of Science and Engineering, James Cook University, Townsville, 4811, Australia
[b] The Ferrier Research Institute, Victoria University of Wellington, Wellington, 6012, New Zealand
[c] Environmental Research Institute, School of Science, University of Waikato, Tauranga, 3110, New Zealand

ARTICLE INFO

Keywords:
Seaweed
Ulva
Sulfated polysaccharide
Ulvan
Rheology
Multivariate analysis

ABSTRACT

Green seaweeds of the genus *Ulva* are rich in the bioactive sulfated polysaccharide ulvan. Herein we characterise ulvan from *Ulva* species collected from the Bay of Plenty, Aotearoa New Zealand. Using standardised procedures, we quantified, characterised, and compared ulvans from blade (*U. australis*, *U. rigida*, *U.* sp. B, and *Ulva* sp.) and filamentous (*U. flexuosa*, *U. compressa*, *U. prolifera*, and *U. ralfsii*) *Ulva* species. There were distinct differences in composition and structure of ulvans between morphologies. Ulvan isolated from blade species had higher yields (14.0–19.3 %) and iduronic acid content (IdoA = 7–18 mol%), and lower molecular weight (Mw = 190–254 kDa) and storage moduli (G' = 0.1–6.6 Pa) than filamentous species (yield = 7.2–14.6 %; IdoA = 4–7 mol%; Mw = 260–406 kDa; G' = 22.7–74.2 Pa). These results highlight the variability of the physicochemical properties of ulvan from different *Ulva* sources, and identifies a morphology-based division within the genus *Ulva*.

1. Introduction

Green seaweeds of the genus *Ulva* occur in two distinct morphologies: a flat sheet-like blade form (occasionally in thin ribbons) and a tubular filamentous form (Fig. 1). Filamentous species of *Ulva* were historically considered a separate genus, *Enteromorpha*, until genetic barcoding concluded that these two genera were not distinct evolutionary entities and were, therefore, consolidated into a single genus, *Ulva* (Hayden et al., 2003). Both morphologies flourish under high nutrient conditions, resulting in blooms or 'green tides' in extreme cases (Ye et al., 2011). Rapid and resilient growth make species of *Ulva* ideal candidates for the bioremediation of nutrient-rich wastewater, such as that produced by land-based aquaculture of shellfish and finfish (Bolton, Robertson-Andersson, Shuuluka, & Kandjengo, 2009; Lawton, Mata, de Nys, & Paul, 2013; Nardelli, Chiozzini, Braga, & Chow, 2019). Applied at a large scale, *Ulva* bioremediation produces a high-quality monoculture of biomass with a biochemical profile that is suitable for the development of valuable bio-products (Glasson, Sims, Carnachan, de Nys, & Magnusson, 2017). Notably, both blade and filamentous *Ulva* are established food products sold as "Aosa" and "Aonori", respectively (Holdt & Kraan, 2011; McHugh, 2003; Ohno, 1993). A key feature of *Ulva* is the high content of soluble fibre, predominantly as the cell wall sulfated polysaccharide ulvan, with desirable biological activities and rheological properties (Alves, Sousa, & Reis, 2013; Kidgell, Magnusson, de Nys, & Glasson, 2019; Lahaye & Robic, 2007).

Ulvan is a heterogeneous rhamnose-rich sulfated polysaccharide that forms weak gels (Haug, 1976; Lahaye & Axelos, 1993). The polysaccharide is characterised by repeat disaccharides of 3-sulfated rhamnose 1,4-linked to either glucuronic acid (ulvanobiouronic acid, A_{3s}), iduronic acid (ulvanobiouronic acid, B_{3s}), or xylose (ulvanobioses, U_{3s}) (Lahaye & Robic, 2007). These assignments, and indeed the majority of research on ulvan, has been conducted on species with the blade morphology (see: Alves et al. (2013); Kidgell et al. (2019); Lahaye and Robic (2007)), while research into the detailed structure of ulvans from filamentous species of *Ulva* is lacking (notable exceptions include: Chattopadhyay et al., 2007; Qi, Huang et al., 2012; Qi, Mao et al., 2012; Tabarsa, You, Dabaghian, & Surayot, 2018; Yu, Li, Du, Mou, & Wang, 2017). In particular, publications characterising ulvans from

* Corresponding author.
E-mail addresses: joel.kidgell@my.jcu.edu.au (J.T. Kidgell), susie.carnachan@vuw.ac.nz (S.M. Carnachan), marie.magnusson@waikato.ac.nz (M. Magnusson), rebecca.lawton@waikato.ac.nz (R.J. Lawton), ian.sims@vuw.ac.nz (I.M. Sims), simon.hinkley@vuw.ac.nz (S.F.R. Hinkley), rocky.denys@jcu.edu.au (R. de Nys), christopher.glasson@waikato.ac.nz (C.R.K. Glasson).

https://doi.org/10.1016/j.carbpol.2021.118010
Received 28 January 2021; Received in revised form 10 March 2021; Accepted 27 March 2021
Available online 2 April 2021

filamentous species of *Ulva* rarely quantify iduronic acid content (Zhong et al., 2020), limiting the extent to which the composition of these ulvans can be compared to those from blade species or between filamentous species (Kidgell et al., 2019). In any case, the structure and composition of ulvan, that is, the constituent sugars, the molecular weight and dispersity, the degree of sulfation, and the content of ulvan within individual *Ulva* samples, varies substantially in the literature (Kidgell et al., 2019).

Variation in the composition and structure of ulvans is due to biological (e.g. *Ulva* species (Shanmugam, Ramavat, Mody, Oza, & Tewari, 2001), holobiont (microbial) community structure (Singh & Reddy, 2014)), environmental (e.g. location (Lahaye et al., 1999), seasonal (Robic, Sassi, Dion, Lerat, & Lahaye, 2009)), and methodological factors (Glasson et al., 2017; Kidgell et al., 2019; Robic, Sassi, & Lahaye, 2008; Yaich et al., 2013). These sources of variation in turn influence the bioactivity and physical properties (e.g. rheology) of the extracted polysaccharide. While the natural variations due to biological and environmental factors are difficult to control, except through controlled cultivation, variability due to methodology can be minimised through the use of standardised procedures. Therefore, the current study used an optimised extraction protocol (Glasson et al., 2019), industry-standard analytical techniques (Pettolino, Walsh, Fincher, & Bacic, 2012) and an optimised rheology protocol (Lahaye & Axelos, 1993; Lahaye, Ray, Baumberger, Quemener, & Axelos, 1996) to compare the yield, composition and structure, and rheological properties of ulvan from *Ulva* species collected and/or cultivated in the Bay of Plenty, Aotearoa New Zealand. Our working hypothesis was that; as ulvan is a structural polysaccharide, the physicochemical properties of ulvan will differ between structurally distinct *Ulva* morphologies.

This study was conducted with the broader aim of selecting target species of *Ulva* for cultivation based on the physicochemical properties of the bioactive polysaccharide ulvan. To achieve this goal, the physicochemical properties of ulvan isolated from different *Ulva* species and morphologies were compared. We determined the yield, constituent sugars, content of sulfate esters, molecular weight distribution, and the rheological properties of ulvans from blade (*U. australis*, *U. rigida*, *U.* sp. B and *U.* sp.) and filamentous (*U. compressa*, *U. flexuosa*, *U. prolifera*, and *U. ralfsii*) *Ulva* species. FTIR and NMR spectroscopy were used to confirm the presence of characteristic ulvan functionality and disaccharides, respectively. Multivariate techniques were then applied to distinguish groupings of similar ulvans based on physicochemical properties of the ulvan from different species and morphologies.

2. Methods

2.1. Materials

The following were purchased from Sigma-Aldrich: glucuronic acid (>98 %, #G5269), sodium tetraborate (99.998 %, #229946), *m*-hydroxydiphenyl (85 %, #262250), concentrated sulfuric acid (ACS, 95–98 %, #258105), boric acid (#B6768), calcium chloride (>99 %, #223506), sodium nitrate (>99.0 %, #S5506), sodium azide (>99 %, #S2002), methanolic HCl (#90964), L-fucose (#F2252), L-rhamnose (#3875), L-arabinose (#10839), D-galactose (#0750), D-glucose (#8270), D-glucosamine (#G4875), D-mannose (#2069), D-xylose (#95729), D-ribose (#7500), D-galacturonic acid (#73960), and D-glucuronic acid (#5269). Other reagents were sourced as follows: trifluoroacetic acid (Synthesis grade, Scharlau, Spain, #AC31420100), sodium chloride (AJAX FineChem, Thermo Fisher Scientific, New Zealand, #AJA465), sodium hydroxide (50 % w/w, Fisher Scientific, Thermo Fisher Scientific, New Zealand, #SS254), anhydrous sodium acetate (Carlo Erba, France, #366377), deuterium oxide (99.9 %, Cambridge Isotope Laboratories, USA, #DLM-4), and L-iduronic acid (Carbosynth, UK, #MI08102).

2.2. Extraction and purification of ulvan

2.2.1. Algae collection & cultivation

Nine morphologically distinct blade and filamentous *Ulva* samples were collected between October 2018 and April 2019 from the Bay of Plenty region, Aotearoa New Zealand (37°42'S, 176°18'E; Fig. S1; See online dataset for details) under Ministry for Primary Industries University of Waikato Special Permit 560. Samples were identified to species level by DNA barcoding by Lawton et al. (Lawton, Sutherland, Glasson, & Magnusson, 2021), and found to consist of seven distinct species (*Ulva australis*, *U. rigida*, *U.* sp. B, *U. compressa*, *U. flexuosa*, *U. prolifera*, *U. ralfsii* [syn. *U.* sp. 5]) and one sample that did not amplify successfully so is referred to as "*Ulva* sp.".

The nine *Ulva* samples were cleaned of epiphytes and rinsed in salt water before being cultivated or extracted. Cultivation was attempted on all nine *Ulva* samples to increase biomass for ulvan extraction, however, *Ulva* sp. was unable to be cultivated. Three of the *Ulva* samples (*U.* sp. B, *U.* sp., *U. ralfsii*) had sufficient wild harvested biomass to extract ulvan after some biomass was taken for cultivation. *Ulva* was cultivated as reported previously (Lawton, Sutherland, Glasson, & Magnusson, 2021). Briefly, cultivation was carried out in 20 L buckets at a density of 1 g fresh weight L^{-1} and a temperature of 18–20°C in sea water with the addition of F/2 nutrients (Cell-Hi F2P, Varicon Aqua Solutions UK, 0.1 g L^{-1}) under bright white LED (1200 mm J Series T8 LED tubes producing 1800 lm of 4000−4500 K light) lights on a cycle of 12 h/12 h light/dark. Biomass was harvested every 7 days and spun to remove excess water. After restocking, excess biomass was frozen at −18 °C until a sufficient supply was produced for ulvan extraction. Frozen biomass was freeze-dried, milled using a domestic blender, and stored over silica gel until extraction.

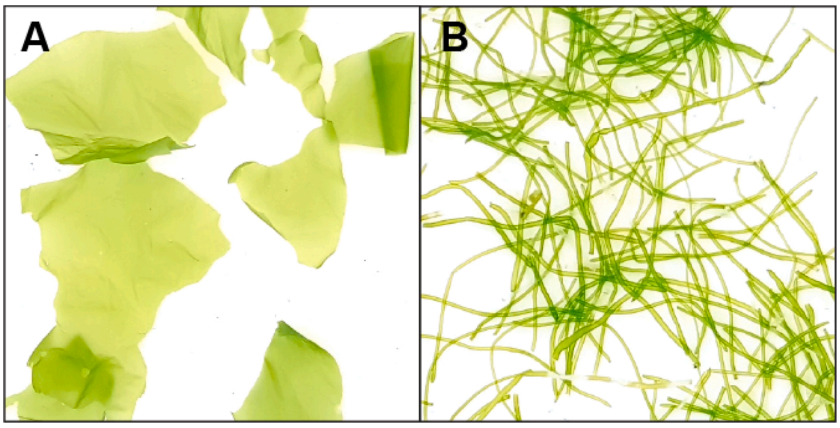

Fig. 1. Characteristic blade (**A**) and filamentous (**B**) morphologies of *Ulva* collected from the Bay of Plenty, Aotearoa New Zealand.

Table 1
Purified ulvan composition: details of the *Ulva* biomass from which ulvan was extracted and purified, the yield (of purified ulvan) obtained, the sulfate and protein content and the ratio of rhamnose to the sum of glucuronic acid, iduronic acid and xylose.

Ulva details			Yield	Composition		
Ulva species	Biomass source	Morphology	Ulvan (% dw)[a]	$\%SO_4^{2-}$[b]	%Protein [c]	[Rha] : [GlcA + IdoA + Xyl][d]
australis	Cultivated	Blade	6.5	16.9 ± 1.1	0.8	1.0
rigida	Cultivated	Blade	5.7	15.2 ± 0.3	0.6	1.1
sp.	Wild harvest	Blade	6.3	16.5 ± 0.7	1.3	1.0
sp. B (cult.A)	Cultivated	Blade	9.5	9.9 ± 0.9	0.7	1.0
sp. B (cult.B)	Cultivated	Blade	8.3	10.4 ± 0.5	0.5	1.1
sp. B (wild)	Wild harvest	Blade	8.0	13.1 ± 1.1	0.3	1.0
compressa	Cultivated	Filamentous	3.3	7.5 ± 0.8	1.2	1.0
flexuosa	Cultivated	Filamentous	7.3	12.2 ± 0.5	1.5	1.3
prolifera	Cultivated	Filamentous	6.6	9.4 ± 0.5	0.7	1.5
ralfsii (cult.)	Cultivated	Filamentous	4.1	7.7 ± 0.4	0.9	0.9
ralfsii (wild)	Wild harvest	Filamentous	4.3	9.8 ± 0.4	0.7	0.9

[a] % dry weight (dw) biomass.
[b] Average of triplicate (±S.D.).
[c] Estimated from conversion factor of 5 (%N x 5).
[d] Ratio of mol% of rhamnose to sum of glucuronic acid, iduronic acid and xylose.

2.2.2. Ulvan extraction

Ulvan was extracted using an optimised extraction procedure (Glasson et al., 2019). A stirred suspension of milled *Ulva* biomass (40 g dry weight) in dilute H_2SO_4 (1 L, pH 2.92) was heated at 90 °C for 90 min. The extract was then separated from the biomass by filtration through 50 μm mesh followed by centrifugation (20 min, 3000 *g*) to remove ultrafine particulate material prior to neutralisation with 2 M NaOH. The extract was then concentrated (10×) by ultrafiltration (ÄKTA flux 6 fitted with a Xampler 10,000 Da NMWC cartridge filter), diafiltered with Type 1 water until the permeate conductivity was ≤20 μS cm^{-1} and freeze dried to yield "crude ulvan" (Table S1).

These crude ulvans containing residual protein and other polysaccharides were characterised in the same manner as the purified ulvan (Table S1). However, four samples (*U. ralfsii* (wild), *U. rigida, U. australis*, and *U. flexuosa)* had insufficient quantities of crude ulvan for characterisation of both crude and purified material. Therefore, only the characterisation of the purified ulvans is explored in detail in the results and discussion.

2.2.3. Purification & fractionation

Crude ulvan was dissolved overnight in Type 1 water at a concentration of 1 % w/w and filtered by vacuum filtration (Filtech, 453) prior to purification by anion exchange chromatography (AEC) using an ÄKTA pure 150 L coupled with a single wavelength (280 nm) UV detector and fraction collector. The ulvan solution was loaded onto an equilibrated (Type 1 water, 5 column volumes (CV); 2 M NaCl, 5 CV; Type 1 water, 5 CV) XK 50/30 column (GE Healthcare Life Sciences) packed with Q Sepharose XL media (bed height =24.5 cm). The column was eluted using a stepwise gradient of NaCl (0 M, 2 CV; 0–1 M, 4 CV; 1–2 M, 1.2 CV; 2 M, 3 CV) at a flow rate of 20 mL min^{-1}. A chromatogram was produced by colorimetric analysis of collected fractions (13 mL) for uronic acid using the *m*-hydroxybiphenyl method with glucuronic acid as standard (van den Hoogen et al., 1998). Fractions containing uronic acid that did not overlap the major peak in the UV trace (attributed to protein and other chromophore containing impurities) were pooled and concentrated by diafiltration with Type 1 water (ÄKTA flux 6 system fitted with a 10,000 Da NMWC filter, UFP-10-E-4 × 2 MA) until permeate conductivity was <5 μS cm^{-1} and then freeze dried to yield "purified ulvan".

Ulvan was successfully extracted and purified from eight cultivated samples and from the wild harvested biomass of three samples (*U.* sp. B, *U.* sp., *U. ralfsii*), resulting in a total of eleven purified ulvans (Table 1). *Ulva* sp. B and *U. ralfsii* both had ulvans extracted and purified from wild harvested and cultivated biomass (Table 1). Two of the *Ulva* samples collected and cultivated were later identified as *U.* sp. B, so were named "*U.* sp. B (cult.A)" and "*U.* sp. B (cult.B)".

2.3. Chemical composition

2.3.1. Elemental characterisation

Elemental analysis (% C, H, N, S; n = 1) and ash content (% w/w) of ulvans were measured commercially by OEA labs (www.oealabs.com, Callington, UK). Percent oxygen was calculated as % O = 100 – Σ(C, H, N, S, ash), where C, H, N, S, and ash are expressed as a percentage of the total mass. Sulfate content was measured using the turbidimetric assay (Craigie, Wen, & van der Meer, 1984). Protein content was estimated from the N content using the nitrogen-to-protein conversion factor of 5 (% N x 5) (Angell, Mata, de Nys, & Paul, 2016).

2.3.2. Constituent sugar composition

Constituent sugar composition was determined by high-performance anion-exchange chromatography with pulsed amperometric detection (HPAEC-PAD) after hydrolysis of the polysaccharides to their component monosaccharides based the methodology of Nep et al. (2016), but with a modified eluant gradient. This methodology was based on the protocol optimised by de Ruiter, Schols, Voragen, and Rombouts (1992) for the analysis of water-soluble uronic acid-containing polysaccharides. Briefly, samples (1 mg) were hydrolysed in duplicate with methanolic HCl (3 M, 500 μL, 80 °C, 18 h), followed by aqueous trifluoroacetic acid (TFA, 2.5 M, 500 μL, 120 °C, 1 h). The resulting hydrolysates were dried, redissolved in Type 1 water (1 mL), and diluted to 50 μg mL^{-1}. Aliquots (20 μL) of the hydrolysates were analysed on a CarboPac PA-1 (4 × 250 mm) column equilibrated in 20 mM NaOH and eluted with a simultaneous gradient of NaOH (20 mM from 0 to 25 min, 20–100 mM from 25−30 min, 100–200 mM from 30 to 50 min, then held to 60 min) and NaOAc (0 mM until 30 min, 0–500 mM from 30 to 50 min, 500–1000 mM from 50 to 52 min, then held until 60 min) at 30 °C and a flow rate of 1 mL min^{-1}. The sugars were identified from their elution times relative to a standard sugar mix (L-fucose, L-rhamnose, L-arabinose, D-galactose, D-glucose, D-glucosamine, D-mannose, D-xylose, D-ribose, D-galacturonic acid, D-glucuronic acid, and L-iduronic acid), quantified from response calibration curves of each sugar and expressed as μg of the anhydro-sugar (as this is the form of sugar present in a polysaccharide) per mg of sample; the normalised mol% of each anhydro-sugar was also calculated.

2.4. Structural characterisation

2.4.1. NMR & FTIR spectroscopy

Samples of ulvan were dissolved in D_2O at 25 mg mL^{-1}. Acetone (0.4

% v/v) was added as an internal standard to all samples and assigned as the reference peak (31.45 ppm for ^{13}C and 2.225 ppm for ^{1}H). NMR data was collected on a Bruker Avance III 500 operating at a proton frequency of 499.843 MHz running Topspin 2.1 software. Data was collected on a Bruker two channel 5-mm broadband observe nuclei probe (31P-109 Ag) equipped with actively shielded Z-axis gradient coil (303 K). Proton NMR spectra were recorded with a spectral width of 20 ppm, 65,536 complex data points, 30-degree excitation pulse, each with a 1-second delay time and an acquisition time of 3.18 s. Heteronuclear single quantum coherence (HSQC) experiments were carried out using pulse programs supplied with the Bruker manual. The superimposed HSQC plots were calibrated by standardising the intensity of the acetone (0.4 % v/v) added as an internal standard resonance between ulvan spectra. Spectra were processed with a standard exponential weighting function of 0.3 Hz line broadening prior to Fourier transformation. NMR spectra were analysed and processed in Mestranova (Ver. 14.1.1).

FTIR spectra of ulvans were recorded on a Shimadzu IRSpirit with a QATR-detector between wavenumbers 400 and 4000 cm^{-1} with an average of 32 scans. Data were processed in LabSolutions IR software using the built-in smoothing function followed by ATR correction, baseline correction and normalisation around the significant peaks for C—O stretching (~1050 cm^{-1}).

2.4.2. Molecular weight

Molecular weight distributions were determined using size-exclusion chromatography coupled with multi-angle laser light scattering (SEC-MALLS). Samples (5 mg mL^{-1} in 0.1 M $NaNO_3$) were dissolved by heating at 80 °C and then standing at room temperature overnight (~20 h). Soluble material was separated on three columns (TSK-Gel $G5000PW_{XL}$, $G4000PW_{XL}$, and $G3000PW_{XL}$, 300 × 7.8 mm, Tosoh Corp., Tokyo, Japan) connected in series, with a void volume (V_0) of 15 mL and total volume (V_t) of 32 mL, eluting with 0.1 M $NaNO_3$ with 0.02 % NaN_3 (0.5 mL min^{-1}, 60 °C). The eluted material was detected using a variable wavelength detector (280 nm), an SDL7000 MALLS detector (PSS Polymer Standards Service GmbH, Mainz, Germany) and a refractive index monitor. Weight-average molecular weight (Mw), number-average molecular weight (Mn), and dispersity (Đ) were calculated using Win GPC Unichrom software (v8.2.1, PSS Polymer Standards Service) using a refractive index increment, dn/dc, of 0.146 mL g^{-1} (Robic et al., 2008). The angular dependence of light scattering was fitted using a linear Debye plot and molecular weight data fitted using linear regression.

2.5. Rheology

Gelling properties of ulvan from *Ulva* species were determined through dynamic rheological measurements performed using a TA Instruments DHR-1 single-head hybrid rheometer with a temperature-controlled Peltier plate and a steel cone geometry (60 mm diameter, 1° angle). Rheological data were collected using TA TRIOS software (ver. 4.3.0.38388). Experiments were conducted at 20 °C with a solvent trap over the geometry to reduce evaporation. Viscosity was measured on a 2 % w/v ulvan solutions (prior to addition of gel-inducing reagents) with a logarithmic flow sweep using a shear rate range of 500 to 1 s^{-1}. For the gelling experiments, the 2 % ulvan solution was pH-adjusted to 7.5 and heated to 75 °C prior to addition of $CaCl_2$ and H_3BO_3 to final concentrations of 7 and 33 mM, respectively, resulting in a final ulvan concentration of 1.6 % (Lahaye & Axelos, 1993; Lahaye, Ray, Baumberger, Quemener, & Axelos, 1996). To prevent the gel from forming prior to starting measurements, H_3BO_3 was added immediately prior to transferring the ulvan solution to the rheometer plate, and the plate was held at 40 °C while the rheometer geometry (rotating at 1 rad s^{-1}) was lowered onto the ulvan solution. Finally, the geometry movement was stopped, the solvent trap was added, and the temperature adjusted to 20 °C prior to beginning any experiments.

The linear viscoelastic region (LVR) was determined with a constant angular frequency of 1 rad s^{-1} across a displacement of 5×10^{-5} to 0.5 rad and indicated that ulvan gels could not withstand an oscillation displacement (strain) greater than 0.01 rad. A displacement of 0.003 rad was selected for subsequent experiments. Ulvan gel formation was monitored by recording the storage modulus resulting from a constant angular frequency of 1 rad s^{-1} with a displacement of 0.003 rad for 30 min. Mechanical spectra (storage and loss moduli, tan δ, complex viscosity) were recorded once gel formation was complete using a constant strain of 0.003 rad displacement over an angular frequency range of 0.03 to 100 rad s^{-1}, a range which maintained a raw phase angle of ≤175° and therefore did not allow inertial forces to dominate the measurements.

2.6. Data & statistical analysis

The effect of the morphology of *Ulva* on chemical and rheological properties of the extracted ulvan was analysed with a one-factor permutational analysis of variance (PERMANOVA) (Anderson, Gorley, & Clarke, 2008). Morphology was treated as a fixed factor. The PERMANOVA was conducted with 9,999 unrestricted permutations and type III sum of squares. Homogeneity of multivariate dispersions was confirmed with the PERMDISP function. Complete linkage cluster analysis was performed with an associated SIMPROF test using a significance level of 5 %, 20,000 permutations to generate the mean profile, and 9,999 permutations to calculate the statistic. Permutational statistical analyses were performed in Primer v6 (Primer-E Ltd., UK) using a Bray-Curtis similarity matrix on square-root transformed data. Correlation matrices were produced in Statistica for Windows (Ver. 12, Statsoft Inc.). Figures were generated using relevant specialised software listed above, R, or Microsoft Excel 2016 and prepared for publication in Adobe Illustrator (Ver. 24).

3. Results and discussion

The physicochemical properties of eleven ulvans isolated and purified from either blade (*U. australis*, *U. rigida*, *U.* sp. B, and *Ulva* sp.) or filamentous (*U. flexuosa*, *U. compressa*, *U. prolifera*, and *U. ralfsii*) *Ulva* species were assessed. The composition of characteristic ulvan sugars (rhamnose, xylose, glucuronic acid, and iduronic acid) conformed to the expected stoichiometry (~1:1 for [Rha]:[GlcA + IdoA + Xyl]) for all ulvans, except those from *U. flexuosa* (1.3:1) and *U. prolifera* (1.5:1), which had 56 and 60 mol% rhamnose, respectively. In general, blade species of *Ulva* had higher yields of ulvan (14.0–19.3 %) containing a higher iduronic acid content (IdoA = 7−18 mol%), lower average molecular weights (M_w = 190−254 kDa), and lower storage moduli (i.e. gel strength, G' = 0.1–6.6 Pa) than ulvan isolated from filamentous species (yield = 7.2–14.6 %; IdoA = 4−7 mol%; M_w = 260−406 kDa; G' = 22.7–74.2 Pa). The above compositional, structural, and rheological data were assessed in a multivariate context which identified a significant difference between ulvans isolated from filamentous and blade species of *Ulva* (PERMANOVA, pseudo-$F_{1,9}$ = 18.0, $p < 0.005$). The current research highlights the variability of the composition and structure of ulvans from different *Ulva* species, and confirms our hypothesis that the physicochemical properties of ulvans differ between *Ulva* morphologies.

3.1. Yield and composition

There are very few studies in the literature that systematically assess the yield and composition of ulvan from a range of *Ulva* species (notable exceptions include: Shanmugam et al. (2001) and Lahaye et al. (1999)), and none that systematically compare ulvans isolated from blade and filamentous morphologies. In this regard, an average yield of 13.4 ± 4.3 % w/w ulvan was extracted from the *Ulva* biomass (Table S1), with an average recovery after purification of 48.3 ± 7.1 % w/w (Table 1). In general, higher yields of purified ulvans were recorded for blade species

(7.4 ± 1.4 %) than for filamentous species (5.1 ± 1.7 %) (Table 1). The crude yields of ulvan (16.5 ± 2.0 % for blade species and 9.8 ± 3.1 % for filamentous species; Table S1) fall within the range of median crude yields (median 12.0, interquartile range = 6.0–20.0) reported in a recent meta-analysis of ulvans (Kidgell et al., 2019), and indicate that blade *Ulva* species have higher contents of ulvan compared to filamentous species. The elemental composition of the ulvans was consistent with previous reports (Tables S1, S2) (Glasson et al., 2017; Kidgell et al., 2020; Shanmugam et al., 2001). Ulvans isolated from blade species had a higher content of sulfate esters than filamentous species with 13.7 ± 2.9 % compared to 9.3 ± 1.8 %, respectively. The degree of sulfation in ulvan has previously been correlated with anticoagulant (Wang, Zhang, Yao, Zhao, & Qi, 2013), antihyperlipidemic (Qi & Sheng, 2015), and anti-viral (Lopes et al., 2017) activity. These results suggest that ulvans isolated from blade and filamentous species of *Ulva* may have different bioactivities (Leiro, Castro, Arranz, & Lamas, 2007; Qi, Huang et al., 2012; Qi, Mao et al., 2012; Shao, Pei, Fang, & Sun, 2014; Wang et al., 2013). The degree of sulfation is also likely to affect the solution properties of ulvan (e.g. rheology) (Lahaye, Ray, Baumberger, Quemener, & Axelos, 1996). Importantly, the protein content of the ulvans in this study is low and there is negligible difference in protein content between samples from blade (0.7 ± 0.3 %) and filamentous (1.0 ± 0.4 %) *Ulva* species, as this is another factor that could drive rheological differences (Robic, Sassi et al., 2009).

The constituent sugar compositions of all purified ulvans broadly conformed to the literature definition of ulvan (Kidgell et al., 2019; Lahaye & Robic, 2007). The ulvans were comprised of 38–60 mol% rhamnose, 17–31 mol% glucuronic acid, 6–22 mol% xylose and 4–18 mol% iduronic acid (Fig. 2, Table S3, Figs. S2, S3). Additionally, a large proportion of galactose (10–16 mol%) was present in ulvans from *U. ralfsii*, and as a minor component in all other ulvans (Tables S3, S4). Notably, ulvans from filamentous species had a lower proportion of acidic to neutral monosaccharides (~0.4:1) compared to those isolated from blade species (~0.6:1). Of particular note is the low proportion of iduronic acid in ulvans isolated from filamentous species (6 ± 1 mol%) relative to ulvans isolated from blade species (12 ± 4 mol%) (Fig. 2). Within this study, ulvan from *U. rigida* had the highest iduronic acid content with 18 mol%, closely followed by ulvans from *U.* sp. B with 11–15 mol% (Fig. 2). An iduronic acid content of 18 mol% (116 μg mg^{-1}; Table S3) is the highest recorded for ulvan in the literature to date (Kidgell et al., 2019). High contents of iduronic acid in ulvans extracted from other blade *Ulva* species, *U. armoricana* (15 mol% (Paradossi, Cavalieri, & Chiessi, 2002) and ~11 mol% (Robic, Sassi et al., 2009)), and *U. ohnoi* (10 mol% (Glasson et al., 2017)) have also been reported. While the effect that iduronic acid content has on ulvan and its function as a cell wall polysaccharide is unclear, high contents are associated with *Ulva* species with blade morphology.

There were several ulvans with sugar compositions that substantially deviate from median literature values (Kidgell et al., 2019). Specifically, ulvans isolated from *U. flexuosa* and *U. prolifera* had high proportions of rhamnose (56 and 60 mol%, respectively), and ulvans from *U. ralfsii* contained high proportions of galactose (10 and 16 mol%) (Fig. 2, Tables S3, S4). The high content of rhamnose in *U. flexuosa* and *U. prolifera* is an interesting result as ulvan is considered to be comprised of rhamnose-containing disaccharides (Lahaye & Robic, 2007). Based on this assumption, the ratio of rhamnose to the sum of glucuronic acid, iduronic acid and xylose (i.e. Rha:[GlcA + IdoA + Xyl]) is theoretically 1:1. Indeed, this ratio is consistent for almost all of the ulvans in this study (ranging from 0.9 to 1.1:1), however, ulvans from *U. flexuosa* and *U. prolifera* had ratios of 1.3:1 and 1.5:1, respectively (Table 1). The excess rhamnose present in these samples may exist as repeat units interspaced between conventional disaccharides, as branching chains, or possibly as a separate repeating rhamnan, related to those found in green seaweeds of the order Ulotrichales, *Gayralia oxsperma* and *Monostroma latissimum* (Cassolato et al., 2008; Lee, Yamagaki, Maeda, & Nakanishi, 1998; Li et al., 2011). Interestingly, despite the high proportions of galactose found in ulvans from filamentous *U. ralfsii*, the Rha:[GlcA + IdoA + Xyl] ratio for both was 0.9:1 (Table 1). A ratio that is also consistent with galactose being either interspaced between the conventional disaccharides of ulvan, as branching chains, or as part of a separate galactan (Castro et al., 2009; Farias et al., 2008). Further structural investigation via linkage analysis and NMR is required to ascertain the origin of the excess rhamnose and high galactose detected in the sugar analysis of ulvans from *U. flexuosa* and *U. prolifera*, and *U. ralfsii*, respectively.

3.2. Structure and rheology

3.2.1. NMR spectroscopy

The ^{1}H and ^{1}H-^{13}C HSQC spectra of purified ulvans from blade and filamentous species of *Ulva* suggest structural differences between the morphologies (Figs. 3–5). Ulvans from blade species have fewer and

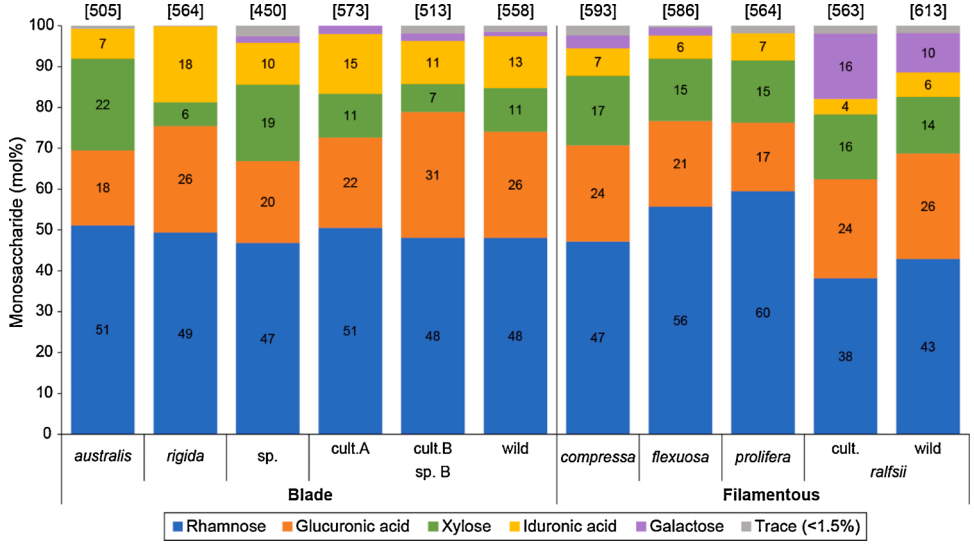

Fig. 2. Constituent monosaccharide composition (mol%) of purified ulvans, categorised by *Ulva* morphology, species, and, for *U.* sp. B and *U. ralfsii*, biomass source. For visual clarity, monosaccharides less than 1.5 mol% were grouped as 'Trace' – full data in Table S3. The total sugar content (μg mg^{-1}) of each ulvan is presented at the top of the respective column in square brackets [].

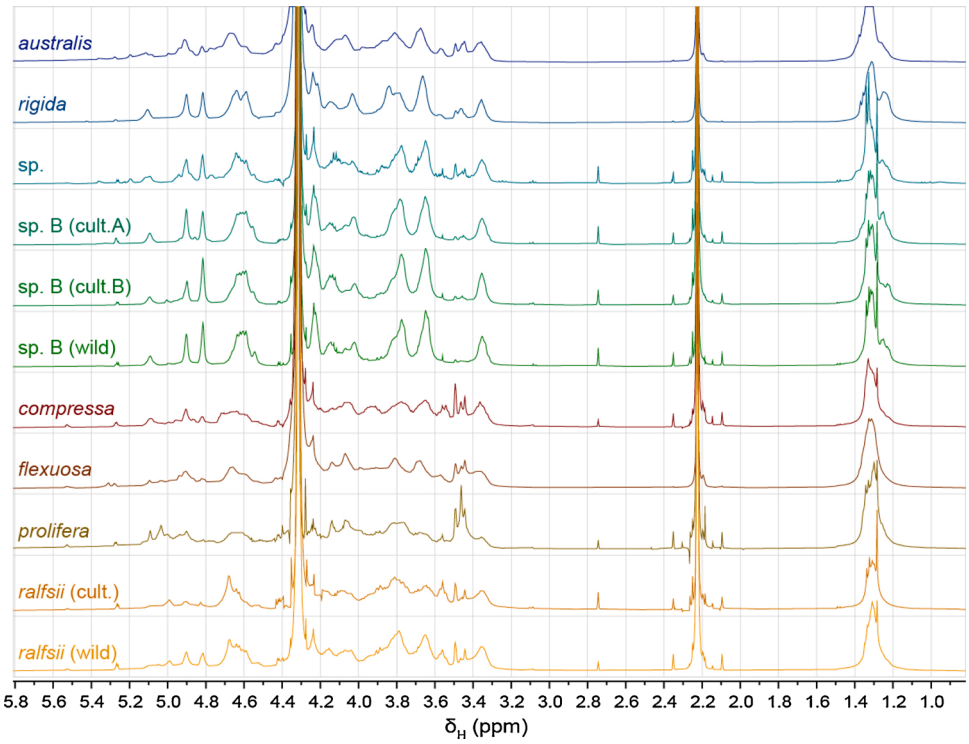

Fig. 3. ^{1}H spectrum of purified ulvans from blade (blue-green) and filamentous (red-yellow) *Ulva* species. Chemical shifts relative to acetone (2.225 ppm).

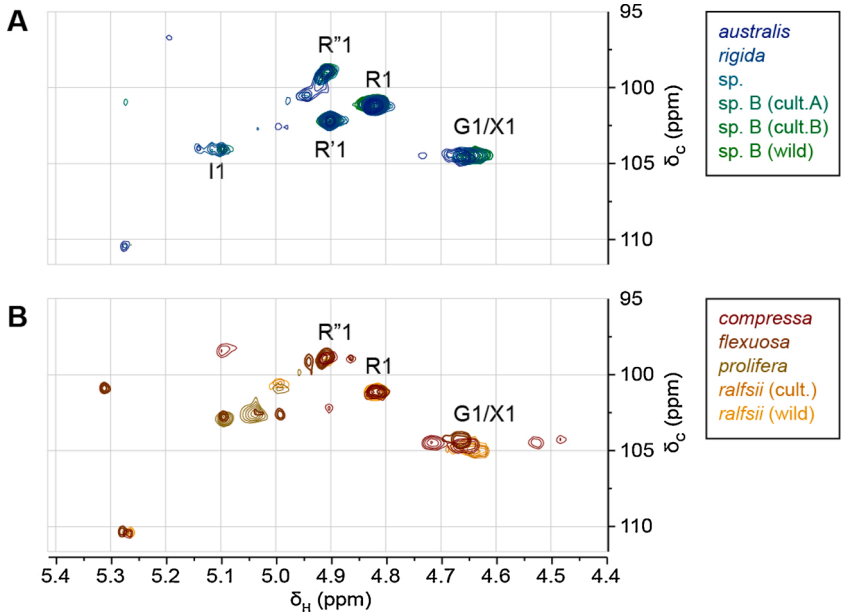

Fig. 4. The anomeric region of superimposed ^{1}H-^{13}C HSQC spectra highlighting the structural difference of ulvans from (**A**) blade and (**B**) filamentous *Ulva* species. Chemical shifts relative to acetone at 31.45 and 2.225 ppm for ^{13}C and ^{1}H, respectively. Labels and numbers correspond to carbon/proton coupling pair of ulvan units outlined in Table 2.

more highly resolved peaks compared to ulvans from filamentous species. This pattern in the 1H NMR may be explained by ulvans isolated from blade species of Ulva containing a high proportion of repeating saccharide structural-moieties, while ulvans from filamentous species are more heterogeneous in structure displaying greater signal complexity (Fig. 3). Almost all the peaks from ulvans of blade species can be identified by comparison with the literature (Table 2). Within the anomeric region (^{13}C ~95–105 ppm/^{1}H ~4.6–5.1, ppm), there are resonances consistent with A_{3S} and U_{3S} disaccharides in ulvans from both blade and filamentous species (Fig. 4, Table 2). Resonances for B_{3S} disaccharides are also detected in ulvans from blade species (Fig. 4A), but not in the spectra of ulvans from filamentous species (Fig. 4B). A lack of anomeric resonances associated with the B_{3S} disaccharide is consistent with the lower content of iduronic acid detected in ulvans from filamentous species (See Section 3.1). Individual HSQC plots further support the constituent sugar analysis (Figs. S5–10). For example, strong resonances are detected for R"1 and R'1 for ulvans high in xylose (*U. australis*, Fig. S5A) and iduronic acid (*U. rigida*, Fig. S5B),

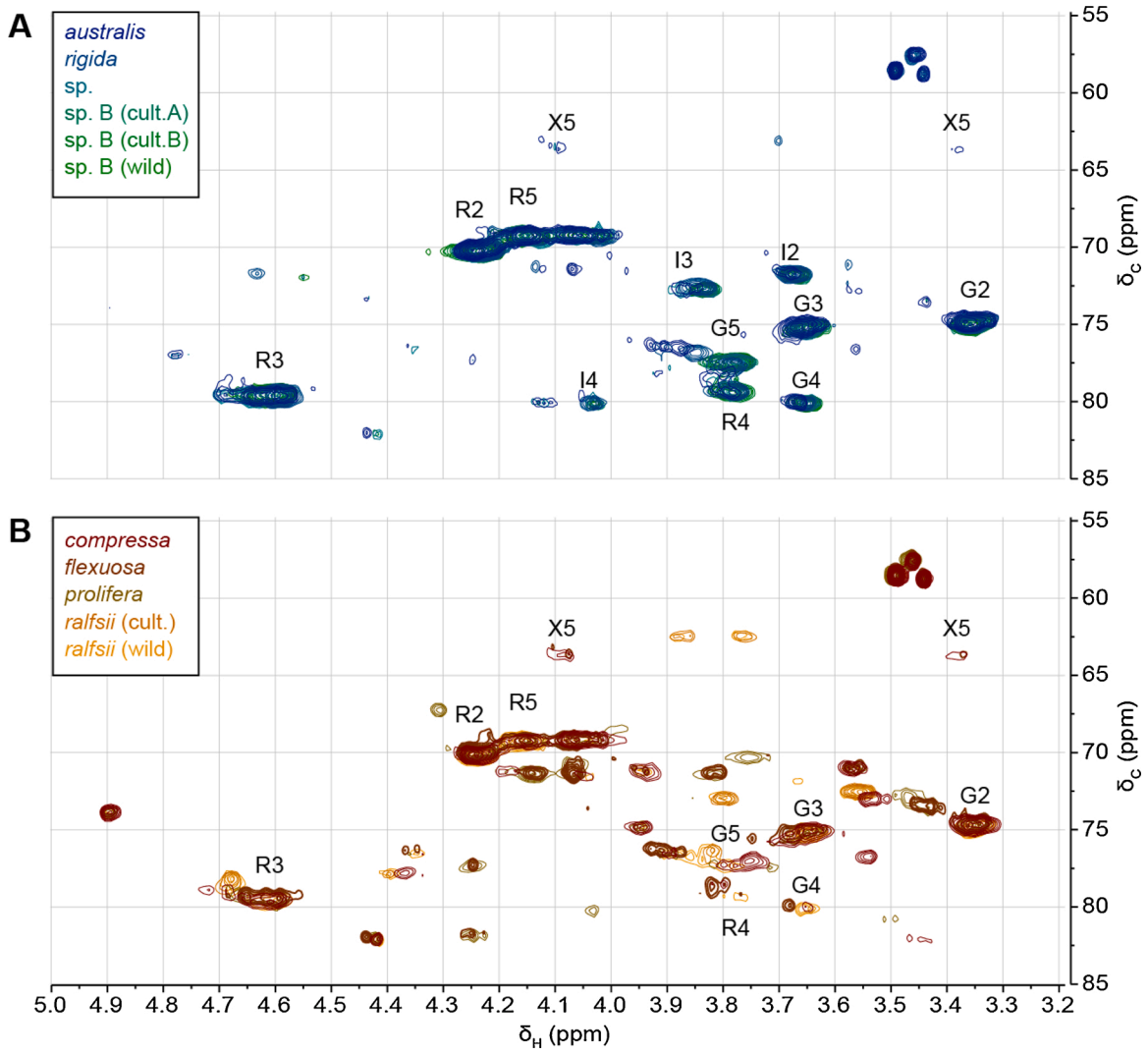

Fig. 5. Non-anomeric region of superimposed ^{1}H-^{13}C HSQC spectra highlighting the structural difference of ulvans from (**A**) blade and (**B**) filamentous *Ulva* species. Chemical shifts relative to acetone at 31.45 and 2.225 ppm for ^{13}C and ^{1}H, respectively. Labels and numbers correspond to carbon/proton coupling pair of ulvan units outlined in Table 2 – note that many resonances from B_{3S} and U_{3S} overlap with A_{3S} so are not specifically listed.

Table 2
Ulvan disaccharide units, assigned labels, and approximate chemical shifts based on references indicated; rounded chemical shift values are given as peaks from different ulvans vary.

Diads[a]	Units	Label	Chemical shift (ppm)[b]						Reference
			C1/H1	C2/H2	C3/H3	C4/H4	C5/H5	C6/H6	
A_{3S}	[→4)-*β*-D-GlcpA-(1→	G	104.5/ 4.65	75.0/ 3.35	75.0/ 3.65	80.0/ 3.65	77.0/ 3.80	–	de Carvalho et al. (2018), de Freitas et al. (2015), Lahaye, Inizan, and Vigouroux (1998)
	4)-*α*-L-Rhap3S-(1→]	R	101.0/ 4.80	70.0/ 4.25	79.0/ 4.60	79.0/ 3.80	69.0/ 4.15	18.0/ 1.30	de Carvalho et al. (2018), de Freitas et al. (2015), Lahaye et al. (1998)
B_{3S}	[→4)-*β*-D-IdopA-(1→	I	104.0/ 5.10	72.0/ 3.70	73.0/ 3.85	80.0/ 4.00	–	–	de Carvalho et al. (2018), Lahaye et al. (1998)
	4)-*α*-L-Rhap3S-(1→]	R'	102.0/ 4.90	70.0/ 4.25[c]	79.0/ 4.60[c]	79.0/ 3.80[c]	69.0/ 4.15[c]	–	Adrien et al. (2017), de Carvalho et al. (2018), Lahaye et al. (1998)
U_{3S}	[→4)-*β*-D-Xyl-(1→	X	104.5/ 4.65	75.0/ 3.35[d]	75.0/ 3.65[d]	75.0/ 3.65[d]	64.0/ 3.40 64.0/ 4.10	–	de Carvalho et al. (2018), de Freitas et al. (2015), Lahaye et al. (1998)
	4)-*α*-L-Rhap3S-(1→]	R"	99.0/ 4.90	70.0/ 4.25[c]	79.0/ 4.60[c]	79.0/ 3.80[c]	69.0/ 4.15[c]	–	de Carvalho et al. (2018), de Freitas et al. (2015), Lahaye et al. (1998)

[a] Nomenclature for disaccharide units follows (Lahaye & Robic, 2007).
[b] Chemical shifts relative to acetone at 31.45 and 2.225 ppm for ^{13}C and ^{1}H, respectively.
[c] Resonance peaks overlap with R.
[d] Resonance peaks overlap with G.

respectively. There are also a series of unassigned resonances detected in ulvans isolated from filamentous species in the region of ^{13}C 100−103 ppm/^{1}H 5.0–5.1 ppm that are absent in those isolated from blade species (Fig. 4, Table 2). Some of these resonances could result from deshielding of the xylose or glucuronic acid anomeric carbons due to the presence of a 2-sulfate (Lahaye et al., 1999), however, further research is required for conclusive assignment. The greater complexity in resonances of ulvans isolated from filamentous species is also detected in the non-anomeric region.

Within the non-anomeric region of the ^{1}H-^{13}C HSQC, the resonances for the A_{3S} and U_{3S} disaccharides can be identified in the spectra of ulvans from both blade and filamentous species of *Ulva* (Table 2). Similar to the anomeric region, resonances for the B_{3S} disaccharide are detected in ulvans from blade species (Fig. 5A) yet are not detected for ulvans from filamentous species (Fig. 5B). Furthermore, a series of resonances between ^{13}C 70-75 ppm/^{1}H 3.4–3.6 ppm are present in the spectra of ulvans from filamentous but not blade species, and do not appear to be identified in the ulvan literature. In the spectra of the galactose-rich ulvans isolated from *U. ralfsii* there are two unidentified resonances at ^{13}C 62.5/^{1}H 3.75 ppm and ^{13}C 62.5/^{1}H 3.85 ppm (Fig. 5B; S9). These resonances are in a region similar to previous assignments made for the C6/H6,6' for a galactan isolated from a green alga (Farias et al., 2008) and a sea urchin (Castro et al., 2009). In addition there are three resonances centred at ~^{13}C 57/^{1}H 3.4 ppm that are more intense in ulvans isolated from filamentous species than blade species (Fig. 5). These resonances likely correspond to a methoxy substituent on one of the sugars, such as 3-O-Me rhamnose (Gosselin, Holt, & Lowe, 1964; McKinnell & Percival, 1962; Ogawa, Yamaura, & Maruyama, 1997). The greater complexity of resonances throughout the ^{1}H-^{13}C HSQC NMR for ulvans isolated from filamentous species supports a higher level of structural complexity in these polysaccharides. However, further structural investigation via linkage analysis is required to elucidate the structural differences between ulvans isolated from blade and filamentous species of *Ulva*.

3.2.2. FTIR spectroscopy

Ulvan has a unique FTIR fingerprint region in the range of 1770−600 cm^{-1} due to the presence of absorptions by carboxylic groups (V_{as} C═O, 1650−1600cm^{-1}; V_s CO, 1425−1400 cm^{-}═^{1}) (Robic, Bertrand, Sassi, Lerat, & Lahaye, 2009; Yaich et al., 2017), sulfate ester groups (V_{as} S═O, 1260−1215 cm^{-1}; COS, 850−835 cm——$^{-1}$ and 795−785 cm^{-1}) (Pengzhan et al., 2003; Ray & Lahaye, 1995; Yaich et al., 2017), and sugar ring side groups and glycosidic linkages (C—OH, COC, ~1055 cm^{-}———^{1}) (Pengzhan et al., 2003; Robic, Bertrand et al., 2009; Zhang et al., 2010). The ulvans assessed in this study consistently displayed absorption profiles characteristic of ulvan within the above-mentioned fingerprint region, with minor variations between ulvans detected (Fig. S4, Table S5). In general, the intensities of the sulfate ester (C—OS, 850−835 cm—$^{-1}$ and 795−785 cm^{-1}) absorptions (relative to absorptions not related to these groups) were higher for ulvans isolated from blade species than ulvans from filamentous species. This pattern is consistent with the higher content of sulfate esters in ulvans from blade species of *Ulva* (See Section 3.1). The absorption pattern in the region commonly associated with glycosidic linkages and other pyranose vibrational modes (~1160−900 cm^{-1}) differed between ulvans isolated from blade and filamentous species of *Ulva*. Specifically, the absorbance at ~980 cm^{-1} had a lower intensity relative to the absorbance at ~1040 cm^{-1} in ulvans isolated from filamentous *Ulva*. While the absorption band at 980 cm^{-1} remains unassigned, the feature corresponds with a lower content of sulfate esters in filamentous samples relative to blade samples and thus may arise due to a vibrational mode associated with the presence of sulfate esters. Indeed, desulfation of ulvan isolated from *U. rigida* also resulted in the disappearance of this peak in two independent studies (Castro et al., 2006; Ray & Lahaye, 1995). However, such an assignment needs further confirmation.

3.2.3. Molecular weight

It is difficult to compare molecular weight profiles of polysaccharides between studies as each step leading to quantification (e.g. biomass collection/cultivation/pre-treatment, extraction, isolation, and measurement method employed) affects the molecular weight measured (de Reviers & Leproux, 1993; Glasson et al., 2017; Robic, Sassi et al., 2009; Robic et al., 2008; Shanmugam et al., 2001; Yaich et al., 2014). For example, in a study where ulvans were extracted from a single source of *U. ohnoi* (a blade species) using different biorefinery pre-treatments and extractants, the weight average molecular weight (M_w) of the isolated ulvan varied from 10.5–312 kDa (Glasson et al., 2017). Other studies have reported widely varying molecular weights for ulvans (e.g. 2000 kDa from blade *U. armoricana* (Hardouin et al., 2016), 194 kDa from filamentous *U. intestinalis* (Tabarsa et al., 2018), and 1218 kDa from filamentous *U. prolifera* (Cho, Yang, Kim, & You, 2010)). The use of standardised protocols such as those employed in the current study overcome the issues of extraction and measurement variability, producing ulvans that only differ on the basis of source biomass (i.e. species/morphology/wild harvest/cultivation).

The M_w of purified ulvans assessed in the current study ranged from 190 to 406 kDa, with ulvans from filamentous species (338 ± 52 kDa) being approximately 50 % larger than those from blade species (225 ± 23 kDa). (Table 3, Figs. S11, S12). Similarly, the number average molecular weight (M_n) of ulvans from filamentous species (216 ± 27 kDa) was over double that of ulvans from blade species (102 ± 24 kDa; Table 3). Variation in molecular weight was detected for ulvans extracted from different biomass sources (cultivated vs. wild harvest) of the same *Ulva* species. Ulvans isolated from blade *U.* sp. B only had a minor variation of 36 kDa (218−254 kDa) while ulvans from filamentous *U. ralfsii* varied by 78 kDa (328−406 kDa). The ulvans with highest molecular weight from both species were isolated from the cultivated biomass. This variation highlights the importance of species selection and cultivation conditions on the quality of ulvan products.

3.2.4. Rheology

Ulvan polysaccharides are capable of forming a weak gel with a storage modulus (i.e. gel strength, G') ranging from 5−600 Pa (Lahaye & Axelos, 1993; Lahaye, Ray, Baumberger, Quemener, & Axelos, 1996; Robic, Sassi et al., 2009; Sari-Chmayssem et al., 2019; Yaich et al., 2014). The ulvan gels formed in this study were prepared using a standardised method at pH 7.5 with a final concentration of ulvan, $CaCl_2$ and H_3BO_3 of 1.6 % w/v, 7 mM, and 33 mM, respectively. Under these conditions the ulvans that formed stronger gels did so rapidly on addition of the boric acid at room temperature, impeding accurate measurements. To overcome this issue, we exploited the thermoreversilibility of the ulvan gels (Fig. S13) (Lahaye, Ray, Baumberger, Quemener, & Axelos, 1996; Qiao et al., 2016; Shao, Qin, Han, & Sun, 2014; Yaich et al., 2014) by adding boric acid to the ulvan solution while heated to 75 °C and maintained the Peltier plate at 40 °C while the geometry was lowered into position for measurement. Using this approach, ulvans isolated from filamentous species of *Ulva* consistently produced gels with a higher storage modulus (G' = 22.7–74.2 Pa) compared to ulvans isolated from blade species (G' = 0.1–6.6 Pa) (Fig. 6, Table 3). It should be noted that the storage modulus of the ulvan isolated from *Ulva ralfsii* (wild) of 74.2 ± 2.6 Pa is greater than three standard deviations from the storage moduli of other ulvans and so was considered an outlier and excluded from further analysis.

Gels formed by ulvans from filamentous species (G' = 27.8 ± 5.1 Pa, excluding *U. ralfsii* (wild)) held their shape and resisted light pressure, while the gels formed by ulvans from blade species (G' = 1.8 ± 2.5 Pa) were akin to highly viscous liquids. Indeed, half of the gels formed by ulvans from blade species of *Ulva* had a tan δ > 1, indicating that the gel was more viscous than elastic and could not be considered a gel (Table 3). The higher content of sulfate in ulvans isolated from blade *Ulva* species could potentially impede intramolecular interactions resulting in lower storage moduli compared to ulvans from filamentous

Table 3
Purified ulvan molecular weight and rheological properties: details of the *Ulva* biomass from which ulvan was extracted, the weight average (M_w) and number average (M_n) molecular weight, dispersity (Đ), the storage modulus and tan δ of the ulvan gel, and the viscosity of a 2 % w/v ulvan solution.

Ulva details		Molecular Weight			Rheology		
Ulva species	Morphology	M_w (kDa)	M_n (kDa)	Đ	Storage Modulus (Pa)[a]	Tan δ	Viscosity (mPa s^{-1})[b]
australis	Blade	214	82	2.6	0.4 ± 0.1	1.6	8
rigida	Blade	190	66	2.9	0.1 ± 0.0	4.3	10
sp.	Blade	245	104	2.4	1.3 ± 0.2	0.8	9
sp. B (cult.A)	Blade	218	126	1.7	0.1 ± 0.0	3.8	14
sp. B (cult.B)	Blade	254	114	2.2	2.2 ± 0.1	0.7	13
sp. B (wild)	Blade	229	120	1.2	6.6 ± 1.4	0.3	14
compressa	Filamentous	346	208	1.7	22.7 ± 2.0	0.1	7
flexuosa	Filamentous	352	218	1.6	34.2 ± 1.8	<0.1	10
prolifera	Filamentous	260	185	1.4	24.9 ± 3.1	0.1	7
ralfsii (cult.)	Filamentous	406	259	1.6	29.5 ± 4.2	0.1	10
ralfsii (wild)	Filamentous	328	210	1.6	74.2 ± 2.6	<0.1	9

[a] Average of triplicate values (±SD) recorded at an angular frequency of 10 rad s^{-1}.
[b] Value recorded at a shear rate of 100 s^{-1}.

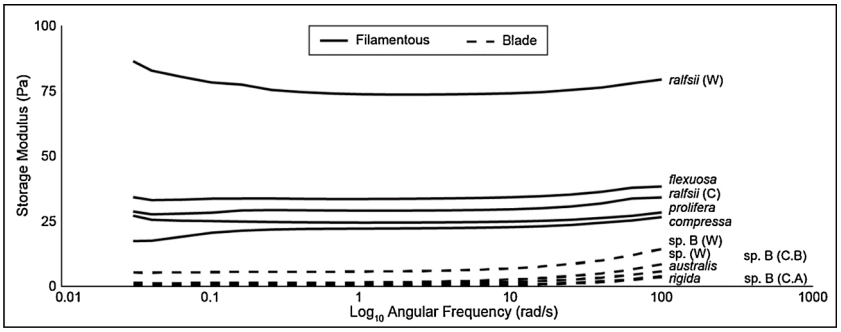

Fig. 6. Storage modulus (gel strength) of purified ulvans in response to a range of rheometer angular frequencies (deformation). Solid lines and dashed lines represent ulvans from filamentous and blade *Ulva* species, respectively. "W" and "C" following a species name indicates whether the biomass was wild harvested or cultivated, respectively; see Table 3 for further details.

species. However, the relationship between ulvan gel formation and sulfate content is unclear and requires further research. Robic, Sassi et al. (2009) found that the gels formed by ulvans varied substantially (G' = 5–600 Pa) when assessing ulvans isolated from different batches of wild harvested *U. rotundata* and *U. armoricana*. The authors attributed the variation in storage moduli to the proportion of high molecular weight ulvan, but also acknowledged that the presence of protein (which ranged from 1.2 to 16.4 % in the ulvans assessed) amplified the storage modulus of the resulting gel. In other studies where the protein content is <5 %, the maximum recorded storage modulus is 250 Pa, but is more consistently below 100 Pa (Lahaye & Axelos, 1993; Sari-Chmayssem et al., 2019; Yaich et al., 2014). Yaich et al. (2014) also reported a decrease in storage modulus with a decrease in molecular weight of ulvans with <5 % protein, as was observed in the current study. Thus, the storage moduli of ulvan gels recorded in the current study (0.1–34.2 Pa) may be at the low end of the reported range for ulvan (G' = 5–600 Pa) due, in part, to low protein content (i.e. high purity of ulvan). In support of this hypothesis is the higher storage moduli of gels formed by crude ulvans, which had higher protein content than purified counterparts (Table S1; Fig. S14). However, crude ulvans also had higher molecular weights than purified ulvans. Further research into the relationship between the storage modulus of ulvan gels, molecular

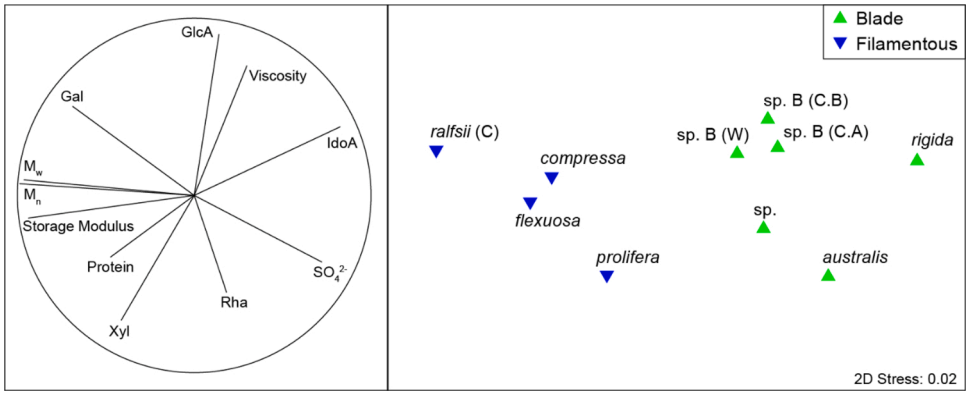

Fig. 7. Multidimensional scaling (MDS) from a square-root transformed Bray-Curtis similarity matrix of the chemical characteristics of the ten ulvans (excluding *U. ralfsii* (wild) as an outlier). Pearson correlation vectors (left plot) influence the distribution of data points (right plot). "W" and "C" following a species name indicates whether the biomass was wild harvested or cultivated, respectively; see Table 3 for further details.

weight, and protein is needed.

3.3. Multivariate synthesis of results

When the composition, structure, and rheological data are considered as a whole, ulvans isolated from blade *Ulva* species are significantly different (pseudo-$F_{1,9} = 18.0$, $p < 0.005$) (Fig. 7) from ulvans isolated from filamentous *Ulva* species. The multivariate dispersions of ulvans from blade and filamentous *Ulva* species did not significantly differ (pseudo-$F_{1,9} = 0.444$, $p = 0.556$), indicating that the significant PERMANOVA result above is due to a difference in ulvans from the two *Ulva* morphologies and not heterogeneous multivariate dispersity of the groups. Ulvans from filamentous and blade species separate on the MDS plot (Fig. 7) due predominantly to the strong positive correlation of large molecular weight and high storage modulus of ulvans of filamentous species, and the high iduronic acid and sulfate content of ulvans from blade species (Table S6). The clustering of ulvans from different morphologies was also significant with 25 % dissimilarity between the two clusters (SIMPROF, $\pi = 1.85$, $p = 0.01$; Fig. S15). The content of glucuronic acid, rhamnose and xylose, and the viscosity of ulvan solutions all had very little effect on the significant distinction of ulvans between *Ulva* morphologies (Fig. 7). The blade and filamentous species analysed here are dispersed throughout the *Ulva* phylogenetic tree (Hayden et al., 2003), and the ulvan physicochemical properties do not reflect the phylogenetic relationship between species. For example, while the physicochemical properties of the ulvans from filamentous *U. compressa* and *U. flexuosa* cause these species to tightly cluster on the MDS plot, these two species are more distantly related phylogenetically than filamentous *U. compressa* and blade *U. australis* (Lawton, Sutherland, Glasson, & Magnusson, 2021), which are widely dispersed on the MDS plot. These findings demonstrate that morphology is driving the significant difference in ulvans and not phylogeny.

The storage modulus of ulvan is strongly positively correlated ($r^2 = 0.9$) with molecular weight (both M_w and M_n), and strongly negatively correlated with iduronic acid ($r^2 = -0.8$) (Table S6). And, in turn, iduronic acid content is strongly negatively correlated with molecular weight ($r^2 = -0.8$). A correlation between molecular weight and storage modulus is intuitive, where an increase in the size of a gel-forming polymer will result in an increase in gel strength due to an increase in intermolecular interactions (Yaich et al., 2014). The correlation of iduronic acid, molecular weight, and storage modulus is somewhat more complicated. Iduronic acid is notoriously acid labile (Conrad, 1980) and its presence in a polysaccharide may contribute to the lower M_w of ulvans due to greater rates of depolymerisation during extraction. In contrast, however, is the principal that the glycosidic linkage of uronic acid to neutral residues is highly acid resistant and the presence of these linkages reduces depolymerisation (BeMiller, 1967). How the acid lability of iduronic acid as a monosaccharide relates to the acid-resistance of its glycosidic linkage is unclear. Iduronic acid also possesses a high degree of conformational freedom (Casu, Petitou, Provasoli, & Sinaÿ, 1988; Hsieh, Thieker, Guerrini, Woods, & Liu, 2016) relative to other monosaccharides (Rees, Morris, Thorn, & Madden, 1982), which may lead to polysaccharide conformations that impede gel formation. Consistent with this hypothesis, ulvans are known to form microbead structures, where the polysaccharide folds back on itself and rolls up into little balls (de Carvalho et al., 2020; Robic, Gaillard, Sassi, Lerat, & Lahaye, 2009). A spherical structure limits the exposed functional areas of the polymer, impeding the strong intramolecular interactions required for high gel strengths, especially given the proposed weak ionic cross-linking mechanism of ulvan gel formation (Lahaye, Ray, Baumberger, Quemener, & Axelos, 1996). Furthermore, models of oligomers of repeat B_{3S} disaccharides (IdoA-Rha3S) have a more helical folded arrangement compared to the more linear structure of oligomers of repeat A_{3S} disaccharides (GlcA-Rha3S) (de Carvalho et al., 2020; Paradossi et al., 2002). The helical arrangement would further limit intramolecular interactions of ulvans rich in B_{3S} disaccharides. Therefore, the sequence and arrangement of disaccharide repeating units in ulvan will likely have a great impact on the gelling capacity of the polymer. Indeed, these studies and our results suggest that the gelling properties of ulvan is diminished in ulvans with high proportions of the B_{3S} disaccharide.

4. Conclusion

The multivariate analysis identified an *Ulva* morphology-based division in the physicochemical properties of isolated ulvans, thus confirming our original hypothesis. The data are compelling when assessed in a multivariate context, which is appropriate as the composition and structure of ulvans drive their rheological properties. Although further validation with ulvans from other species is required to generalise this pattern more broadly, the identification of a morphology-based distinction in ulvan is an important step forward in ulvan research. Not only in characterisation of the under-studied ulvans from filamentous species of *Ulva*, but also in the application of ulvan isolated from cultivated *Ulva* biomass. This research identifies a potential to select an *Ulva* morphology for cultivation to target a desirable property or activity in the resulting ulvan. For example, in the context of this study, ulvan from *U. ralfsii* would be suited for rheological applications. However, further understanding of the structure-activity relationships between ulvans isolated from different species and morphologies are required for species selection based on favourable biological activities. In closing, there is a clear disparity in ulvans from blade and filamentous species of *Ulva*, demonstrating the importance of considering morphology in the selection of *Ulva* species for cultivation with respect to the biotechnical applications of ulvan.

CRediT authorship contribution statement

Joel T. Kidgell: Conceptualisation, investigation, data curation, visualisation, writing – original draft. **Susan M. Carnachan:** Investigation, supervision, writing – original draft. **Marie Magnusson:** Conceptualisation, resources, funding, writing – review and editing. **Rebecca Lawton:** Investigation (algal cultivation), writing – original draft. **Ian M. Sims:** Investigation, writing – original draft. **Simon F.R. Hinkley:** Resources, supervision, writing – review and editing. **Rocky de Nys:** Conceptualisation, resources, funding, supervision, writing – review and editing. **Christopher R.K. Glasson:** Conceptualisation, investigation, supervision, methodology, writing – original draft.

Acknowledgments

The authors would like to thank Peter Randrup for his assistance with sample collection, *Ulva* cultivation and photos, Ari Brandenburg for her assistance in the laboratory work, and Andrew Lewis for his assistance in performing the NMR experiments. We would also like to acknowledge James Cook University and the Australian Government for providing a Research Training Program Scholarship to Joel Kidgell. This research is part of the Entrepreneurial Universities Macroalgal Biotechnologies Programme, jointly funded by the University of Waikato and the Tertiary Education Commission.

Appendix A. Supplementary data

Supplementary material related to this article can be found, in the online version, at doi:https://doi.org/10.1016/j.carbpol.2021.118010.

References

Adrien, A., Bonnet, A., Dufour, D., Baudouin, S., Maugard, T., & Bridiau, N. (2017). Pilot production of ulvans from *Ulva* sp. and their effects on hyaluronan and collagen production in cultured dermal fibroblasts. *Carbohydrate Polymers, 157*, 1306–1314.

Alves, A., Sousa, R. A., & Reis, R. L. (2013). A practical perspective on ulvan extracted from green algae. *Journal of Applied Phycology, 25*(2), 407–424.

Anderson, M. J., Gorley, R. N., & Clarke, R. K. (2008). *Permanova+ for Primer: Guide to software and statistical methods*.

Angell, A. R., Mata, L., de Nys, R., & Paul, N. A. (2016). The protein content of seaweeds: A universal nitrogen-to-protein conversion factor of five. *Journal of Applied Phycology, 28*(1), 511–524.

BeMiller, J. N. (1967). Acid-catalyzed hydrolysis of glycosides. *Advances in Carbohydrate Chemistry and Biochemistry, 22*, 25–108.

Bolton, J. J., Robertson-Andersson, D. V., Shuuluka, D., & Kandjengo, L. (2009). Growing Ulva (Chlorophyta) in integrated systems as a commercial crop for abalone feed in South Africa: A SWOT analysis. *Journal of Applied Phycology, 21*(5), 575–583.

Cassolato, J. E., Noseda, M. D., Pujol, C. A., Pellizzari, F. M., Damonte, E. B., & Duarte, M. E. (2008). Chemical structure and antiviral activity of the sulfated heterorhamnan isolated from the green seaweed *Gayralia oxysperma*. *Carbohydrate Research, 343*(18), 3085–3095.

Castro, M. O., Pomin, V. H., Santos, L. L., Vilela-Silva, A. C., Hirohashi, N., Pol-Fachin, L., et al. (2009). A unique 2-sulfated {beta}-galactan from the egg jelly of the sea urchin Glyptocidaris crenularis: Conformation flexibility versus induction of the sperm acrosome reaction. *The Journal of Biological Chemistry, 284*(28), 18790–18800.

Castro, R., Piazzon, M. C., Zarra, I., Leiro, J., Noya, M., & Lamas, J. (2006). Stimulation of turbot phagocytes by *Ulva rigida* C. Agardh polysaccharides. *Aquaculture, 254*(1), 9–20.

Casu, B., Petitou, M., Provasoli, M., & Sinaÿ, P. (1988). Conformational flexibility: A new concept for explaining binding and biological properties of iduronic acid-containing glycosaminoglycans. *Trends in Biochemical Sciences, 13*(6), 221–225.

Chattopadhyay, K., Mandal, P., Lerouge, P., Driouich, A., Ghosal, P., & Ray, B. (2007). Sulphated polysaccharides from Indian samples of *Enteromorpha compressa* (Ulvales, Chlorophyta): Isolation and structural features. *Food Chemistry, 104*(3), 928–935.

Cho, M., Yang, C., Kim, S. M., & You, S. (2010). Molecular characterization and biological activities of water-soluble sulfated polysaccharides from *Enteromorpha prolifera*. *Food Science and Biotechnology, 19*(2), 525–533.

Conrad, H. E. (1980). The acid lability of the glycosidic bonds of L-iduronic acid residues in glycosaminoglycans. *The Biochemical Journal, 191*(2), 355–363.

Craigie, J. S., Wen, Z. C., & van der Meer, J. P. (1984). Interspecific, intraspecific and nutritionally-determined variations in the composition of agars from *Gracilaria* spp. *Botanica Marina, 27*, 55.

de Carvalho, M. M., de Freitas, R. A., Ducatti, D. R. B., Ferreira, L. G., Gonçalves, A. G., Colodi, F. G., et al. (2018). Modification of ulvans via periodate-chlorite oxidation: Chemical characterization and anticoagulant activity. *Carbohydrate Polymers, 197*, 631–640.

de Carvalho, M. M., Noseda, M. D., Dallagnol, J. C. C., Ferreira, L. G., Ducatti, D. R. B., Gonçalves, A. G., et al. (2020). Conformational analysis of ulvans from *Ulva fasciata* and their anticoagulant polycarboxylic derivatives. *International Journal of Biological Macromolecules, 162*, 599–608.

de Freitas, M. B., Ferreira, L. G., Hawerroth, C., Duarte, M. E. R., Noseda, M. D., & Stadnik, M. J. (2015). Ulvans induce resistance against plant pathogenic fungi independently of their sulfation degree. *Carbohydrate Polymers, 133*, 384–390.

de Reviers, B., & Leproux, A. (1993). Characterization of polysaccharides from *Enteromorpha intestinalis* (L.) link, chlorophyta. *Carbohydrate Polymers, 22*(4), 253–259.

de Ruiter, G. A., Schols, H. A., Voragen, A. G. J., & Rombouts, F. M. (1992). Carbohydrate analysis of water-soluble uronic acid-containing polysaccharides with high-performance anion-exchange chromatography using methanolysis combined with TFA hydrolysis is superior to four other methods. *Analytical Biochemistry, 207*(1), 176–185.

Farias, E., Pomin, V., Valente, A., Nader, H., Rocha, H., & Mourão, P. (2008). A preponderantly 4-sulfated, 3-linked galactan from the green alga *Codium isthmocladum*. *Glycobiology, 18*, 250–259.

Glasson, C. R. K., Donnet, L., Angell, A., Vucko, M. J., Lorbeer, A. J., Vamvounis, G., et al. (2019). Multiple response optimisation of the aqueous extraction of high quality ulvan from *Ulva ohnoi*. *Bioresource Technology Reports, 7*.

Glasson, C. R. K., Sims, I. M., Carnachan, S. M., de Nys, R., & Magnusson, M. (2017). A cascading biorefinery process targeting sulfated polysaccharides (ulvan) from *Ulva ohnoi*. *Algal Research, 27*, 383–391.

Gosselin, C. C., Holt, A., & Lowe, P. A. (1964). Polysaccharides of *Enteromorpha* species. *Journal of the Chemical Society (Resumed)*, 5877–5880.

Hardouin, K., Bedoux, G., Burlot, A.-S., Donnay-Moreno, C., Bergé, J.-P., Nyvall-Collén, P., et al. (2016). Enzyme-assisted extraction (EAE) for the production of antiviral and antioxidant extracts from the green seaweed *Ulva armoricana* (Ulvales, Ulvophyceae). *Algal Research, 16*, 233–239.

Haug, A. (1976). The influence of borate and calcium on the gel formation of a sulfated polysaccharide from *Ulva lactuca*. *Acta Chemica Scandinavica. Series B: Organic Chemistry and Biochemistry, 30*(6), 562–566.

Hayden, H. S., Blomster, J., Maggs, C. A., Silva, P. C., Stanhope, M. J., & Waaland, J. R. (2003). Linnaeus was right all along: *Ulva* and *Enteromorpha* are not distinct genera. *European Journal of Phycology, 38*(3), 277–294.

Holdt, S. L., & Kraan, S. (2011). Bioactive compounds in seaweed: Functional food applications and legislation. *Journal of Applied Phycology, 23*(3), 543–597.

Hsieh, P.-H., Thieker, D. F., Guerrini, M., Woods, R. J., & Liu, J. (2016). Uncovering the relationship between sulphation patterns and conformation of iduronic acid in Heparan sulphate. *Scientific Reports, 6*(1), 29602.

Kidgell, J. T., Glasson, C. R. K., Magnusson, M., Vamvounis, G., Sims, I. M., Carnachan, S. M., et al. (2020). The molecular weight of ulvan affects the in vitro inflammatory response of a murine macrophage. *International Journal of Biological Macromolecules, 150*, 839–848.

Kidgell, J. T., Magnusson, M., de Nys, R., & Glasson, C. R. K. (2019). Ulvan: A systematic review of extraction, composition and function. *Algal Research, 39*, Article 101422.

Lahaye, M., & Axelos, M. A. V. (1993). Gelling properties of water-soluble polysaccharides from proliferating marine green seaweeds (*Ulva* spp.). *Carbohydrate Polymers, 22*(4), 261–265.

Lahaye, M., & Robic, A. (2007). Structure and functional properties of ulvan, a polysaccharide from green seaweeds. *Biomacromolecules, 8*(6), 1765–1774.

Lahaye, M., Cimadevilla, E. A. C., Kuhlenkamp, R., Quemener, B., Lognoné, V., & Dion, P. (1999). Chemical composition and 13C NMR spectroscopic characterisation of ulvans from *Ulva* (Ulvales, Chlorophyta). *Journal of Applied Phycology, 11*(1), 1–7.

Lahaye, M., Inizan, F., & Vigouroux, J. (1998). NMR analysis of the chemical structure of ulvan and of ulvan-boron complex formation. *Carbohydrate Polymers, 36*(2-3), 239–249.

Lahaye, M., Ray, B., Baumberger, S., Quemener, B., & Axelos, M. A. V. (1996). Chemical characterisation and gelling properties of cell wall polysaccharides from species of *Ulva* (Ulvales, Chlorophyta). *Hydrobiologia, 326*(1), 473–480.

Lawton, R. J., Mata, L., de Nys, R., & Paul, N. A. (2013). Algal bioremediation of waste waters from land-based aquaculture using *Ulva*: Selecting target species and strains. *PloS One, 8*(10), Article e77344.

Lawton, R. J., Sutherland, J. E., Glasson, C. R. K., & Magnusson, M. (2021). Selection of temperate *Ulva* species and strains for land-based cultivation and biomass applications. *Algal Research*. Submitted for publication.

Lee, J. B., Yamagaki, T., Maeda, M., & Nakanishi, H. (1998). Rhamnan sulfate from cell walls of *Monostroma latissimum*. *Phytochemistry, 48*(6), 921–925.

Leiro, J. M., Castro, R., Arranz, J. A., & Lamas, J. (2007). Immunomodulating activities of acidic sulphated polysaccharides obtained from the seaweed *Ulva rigida* C. Agardh. *International Immunopharmacology, 7*(7), 879–888.

Li, H., Mao, W., Zhang, X., Qi, X., Chen, Y., Chen, Y., et al. (2011). Structural characterization of an anticoagulant-active sulfated polysaccharide isolated from green alga *Monostroma latissimum*. *Carbohydrate Polymers, 85*(2), 394–400.

Lopes, N., Ray, S., Espada, S. F., Bomfim, W. A., Ray, B., Faccin-Galhardi, L. C., et al. (2017). Green seaweed *Enteromorpha compressa* (Chlorophyta, Ulvaceae) derived sulphated polysaccharides inhibit herpes simplex virus. *International Journal of Biological Macromolecules, 102*, 605–612.

McHugh, D. J. (2003). *A guide to the seaweed industry*. FAO Fisheries Technical Paper. No. 441 (p. 105). Rome: FAO.

Nardelli, A. E., Chiozzini, V. G., Braga, E. S., & Chow, F. (2019). Integrated multi-trophic farming system between the green seaweed *Ulva lactuca*, mussel, and fish: A production and bioremediation solution. *Journal of Applied Phycology, 31*, 847–856. https://doi.org/10.1007/s10811-018-1581-4

McKinnell, J. P., & Percival, E. (1962). The acid polysaccharide from the Green Seaweed, *Ulva lactuca*. *Journal of the Chemical Society*, 2082–2084 (Resumed)(0).

Nep, E. I., Carnachan, S. M., Ngwuluka, N. C., Kontogiorgos, V., Morris, G. A., Sims, I. M., et al. (2016). Structural characterisation and rheological properties of a polysaccharide from sesame leaves (*Sesamum radiatum* Schumach. & Thonn.). *Carbohydrate Polymers, 152*, 541–547.

Ogawa, K., Yamaura, M., & Maruyama, I. (1997). Isolation and identification of 2-O-methyl-l-rhamnose and 3-O-methyl-l-rhamnose as constituents of an acidic polysaccharide of *Chlorella vulgaris*. *Bioscience, Biotechnology, and Biochemistry, 61*(3), 539–540.

Ohno, M. (1993). Cultivation of the green algae *Monostroma* and *Enteromorpha* "*Aonori*". In M. Ohno, & A. T. Critchley (Eds.), *Seaweed cultivation and marine ranching* (pp. 7–16). Jokocuka: Japan International Cooperation Agency.

Paradossi, G., Cavalieri, F., & Chiessi, E. (2002). A conformational study on the algal polysaccharide ulvan. *Macromolecules, 35*(16), 6404–6411.

Pengzhan, Y., Quanbin, Z., Ning, L., Zuhong, X., Yanmei, W., & Zhi'en, L. (2003). Polysaccharides from *Ulva pertusa* (Chlorophyta) and preliminary studies on their antihyperlipidemia activity. *Journal of Applied Phycology, 15*(1), 21–27.

Pettolino, F. A., Walsh, C., Fincher, G. B., & Bacic, A. (2012). Determining the polysaccharide composition of plant cell walls. *Nature Protocols, 7*(9), 1590–1607.

Qi, H., & Sheng, J. (2015). The antihyperlipidemic mechanism of high sulfate content ulvan in rats. *Marine Drugs, 13*(6), 3407–3421.

Qi, H., Huang, L., Liu, X., Liu, D., Zhang, Q., & Liu, S. (2012). Antihyperlipidemic activity of high sulfate content derivative of polysaccharide extracted from *Ulva pertusa* (Chlorophyta). *Carbohydrate Polymers, 87*(2), 1637–1640.

Qi, X. H., Mao, W. J., Gao, Y., Chen, Y., Chen, Y. L., Zhao, C. Q., et al. (2012). Chemical characteristic of an anticoagulant-active sulfated polysaccharide from *Enteromorpha clathrata*. *Carbohydrate Polymers, 90*(4), 1804–1810.

Qiao, L. K., Li, Y. P., Chi, Y. Z., Ji, Y. L., Gao, Y., Hwang, H. M., et al. (2016). Rheological properties, gelling behavior and texture characteristics of polysaccharide from *Enteromorpha prolifera*. *Carbohydrate Polymers, 136*, 1307–1314.

Ray, B., & Lahaye, M. (1995). Cell-wall polysaccharides from the marine green alga *Ulva* "*rigida*" (Ulvales, Chlorophyta). Chemical structure of ulvan. *Carbohydrate Research, 274*, 313–318.

Rees, D. A., Morris, E. R., Thorn, D., & Madden, J. K. (1982). Shapes and interactions of carbohydrate chains. In G. O. Aspinall (Ed.), *The polysaccharides* (pp. 195–290). New York: Academic Press.

Robic, A., Sassi, J. F., & Lahaye, M. (2008). Impact of stabilization treatments of the green seaweed *Ulva rotundata* (Chlorophyta) on the extraction yield, the physico-chemical and rheological properties of ulvan. *Carbohydrate Polymers, 74*(3), 344–352.

Robic, A., Bertrand, D., Sassi, J. F., Lerat, Y., & Lahaye, M. (2009). Determination of the chemical composition of ulvan, a cell wall polysaccharide from *Ulva* spp. (Ulvales, Chlorophyta) by FT-IR and chemometrics. *Journal of Applied Phycology, 21*(4), 451–456.

Robic, A., Gaillard, C., Sassi, J. F., Lerat, Y., & Lahaye, M. (2009). Ultrastructure of ulvan: A polysaccharide from green seaweeds. *Biopolymers, 91*(8), 652–664.

Robic, A., Sassi, J. F., Dion, P., Lerat, Y., & Lahaye, M. (2009). Seasonal variability of physicochemical and rheological properties of ulvan in two *Ulva* species (chlorophyta) from the Brittany coast. *Journal of Phycology, 45*(4), 962–973.

Sari-Chmayssem, N., Taha, S., Mawlawi, H., Guégan, J.-P., Jeftić, J., & Benvegnu, T. (2019). Extracted ulvans from green algae *Ulva linza* of Lebanese origin and amphiphilic derivatives: Evaluation of their physico-chemical and rheological properties. *Journal of Applied Phycology, 31*(3), 1931–1946.

Shanmugam, M., Ramavat, B. K., Mody, K. H., Oza, R. M., & Tewari, A. (2001). Distribution of heparinoid-active sulphated polysaccharides in some Indian marine green algae. *Indian Journal of Marine Sciences, 30*(4), 222–227.

Shao, P., Pei, Y., Fang, Z., & Sun, P. (2014). Effects of partial desulfation on antioxidant and inhibition of DLD cancer cell of Ulva fasciata polysaccharide. *International Journal of Biological Macromolecules, 65*, 307–313.

Shao, P., Qin, M. P., Han, L. F., & Sun, P. L. (2014). Rheology and characteristics of sulfated polysaccharides from chlorophytan seaweeds *Ulva fasciata*. *Carbohydrate Polymers, 113*, 365–372.

Singh, R. P., & Reddy, C. R. K. (2014). Seaweed–microbial interactions: Key functions of seaweed-associated bacteria. *FEMS Microbiology Ecology, 88*(2), 213–230.

Tabarsa, M., You, S., Dabaghian, E. H., & Surayot, U. (2018). Water-soluble polysaccharides from *Ulva intestinalis*: Molecular properties, structural elucidation and immunomodulatory activities. *Journal of Food and Drug Analysis, 26*(2), 599–608.

van den Hoogen, B. M., van Weeren, P. R., Lopes-Cardozo, M., van Golde, L. M., Barneveld, A., & van de Lest, C. H. (1998). A microtiter plate assay for the determination of uronic acids. *Analytical Biochemistry, 257*(2), 107–111.

Wang, X. M., Zhang, Z. S., Yao, Z. Y., Zhao, M. X., & Qi, H. M. (2013). Sulfation, anticoagulant and antioxidant activities of polysaccharide from green algae *Enteromorpha linza*. *International Journal of Biological Macromolecules, 58*, 225–230.

Yaich, H., Amira, A. B., Abbes, F., Bouaziz, M., Besbes, S., Richel, A., et al. (2017). Effect of extraction procedures on structural, thermal and antioxidant properties of ulvan from *Ulva lactuca* collected in Monastir coast. *International Journal of Biological Macromolecules, 105*(Pt 2), 1430–1439.

Yaich, H., Garna, H., Besbes, S., Barthélemy, J.-P., Paquot, M., Blecker, C., et al. (2014). Impact of extraction procedures on the chemical, rheological and textural properties of ulvan from *Ulva lactuca* of Tunisia coast. *Food Hydrocolloids, 40*, 53–63.

Yaich, H., Garna, H., Besbes, S., Paquot, M., Blecker, C., & Attia, H. (2013). Effect of extraction conditions on the yield and purity of ulvan extracted from *Ulva lactuca*. *Food Hydrocolloids, 31*(2), 375–382.

Ye, N.-h., Zhang, X.-w., Mao, Y.-z., Liang, C.-w., Xu, D., Zou, J., et al. (2011). "Green tides" are overwhelming the coastline of our blue planet: Taking the world's largest example. *Ecological Research, 26*(3), 477.

Yu, Y., Li, Y. P., Du, C. Y., Mou, H. J., & Wang, P. (2017). Compositional and structural characteristics of sulfated polysaccharide from *Enteromorpha prolifera*. *Carbohydrate Polymers, 165*, 221–228.

Zhang, Z. S., Wang, F., Wang, X. M., Liu, X. L., Hou, Y., & Zhang, Q. B. (2010). Extraction of the polysaccharides from five algae and their potential antioxidant activity in vitro. *Carbohydrate Polymers, 82*(1), 118–121.

Zhong, R., Wan, X., Wang, D., Zhao, C., Liu, D., Gao, L., et al. (2020). Polysaccharides from marine *Enteromorpha*: Structure and function. *Trends in Food Science & Technology, 99*, 11–20.